FRACTURE TOUGHNESS OF A HIGH-STRENGTH LOW-ALLOY STEEL WELDMENT

ŽILAVOST LOMA ZVARA VISOKOTRDNEGA MALOLEGIRANEGA JEKLA

Jelena Tuma[1], Nenad Gubeljak[2], Borivoj Šuštaršič[1], Borut Bundara[3]

[1]Institute of Metals and Technology, Lepi pot 11, 1000 Ljubljana, Slovenia
[2]University of Maribor, Faculty of Mechanical Engineering, Smetanova 17, 2000 Maribor, Slovenia
[3]Institute of Metals Constructions, Mencingerjeva 7, 1000 Ljubljana, Slovenia
jelena.tuma@imt.si

The use of high-strength low-alloy steels for high-performance structures, e.g., pressure vessels and pipelines, requires often high-strength consumables to produce an overmatched welded joint. This globally overmatched welded joint contains local mis-matched regions, which can affect the unstable fracture behaviour of the welded joint and the welded structure itself. If local mis-matched regions are present in the vicinity of a crack tip, then the fracture toughness of the weld metal can be significantly lower than that of the base metal. In this paper, the influence of the weld-metal microstructure on the fracture behaviour is estimated enabling an evaluation of the resistance to stable crack growth through different microstructures. The lower bound of the fracture toughness for different microstructures was evaluated using a modified Weibull distribution. The results, obtained using specimens with a through thickness crack front, indicated a low fracture toughness, caused by the strength mis-matching interaction along the crack front. In the case of through-the-thickness specimens, at least one local brittle zone (LBZ) or a local soft region is incorporated into the process zone in the vicinity of the crack tip. Hence, an unstable fracture occurred with small stable crack propagation, or without it. Despite the fact that the differences between the impact toughness of the weld metal and the base metal can be insignificant, the fracture toughness of a weld metal can be significantly lower.

Key words: fracture mechanics, welded joint, crack-tip opening displacement, resistance curves

Uporaba visokotrdnih malolegiranih jekel za zelo obremenjene strukture, npr. posode pod pritiskom in cevovode, zahteva uporabo varilnega materiala, ki ustvari zvar z večjo trdnostjo. Taki zvari vsebujejo lokalna področja z mešano trdnostjo, ki lahko vplivajo na nestabilno lomno vedenje zvara in zvarjene strukture. Če mešana področja ležijo v bližini vrha razpoke, je lahko žilavost loma pomembno manjša kot pri osnovnem materialu. V tem delu je ocenjen vpliv mikrostrukture zvara na vedenje pri lomu, kar omogoča oceno odpornosti proti stabilnem širjenju razpoke skozi različne mikrostrukture. Nižja vrednost žilavosti loma je bila ocenjena za različne mikrostrukture z modificirano Weibullovo porazdelitvijo. Rezultati, ki so bili doseženi pri vzorcih z razpoko preko debeline, so pokazali nizko žilavost loma zaradi različne trdnosti vzdolž čela razpoke. V primeru vzorcev z razpoko preko debeline je vsaj eno lokalno krhko področje (LBZ) ali lokalno mehko področje vključeno v procesno področje v bližini vrha razpoke. Zato se je stabilna propagacija razpoke izvršila z majhnim stabilnim širjenjem ali brez njega. Čeprav so majhne razlike med udarno žilavostjo zvara in osnovnega materiala, je lahko žilavost loma zvara pomembno manjša.

Ključne besede: mehanika loma, zvarni spoj, premik vrha odprtja razpoke, krivulje odpornosti

1 INTRODUCTION

Strength-overmatched welded joints are designed to ensure the safe service of a welded structure by keeping the flaws, e.g., planar defects, in an elastic weld metal, while the base metal starts to yield. Such an approach ensures that a welded structure can sustain local plastic deformation, important when temporary overloading or geometrical changes occur. These changes can be caused by temperature variations during a structures service life. The strength-overmatching requirement presents no special problems for steel with yield strength of less than 600 MPa [1], but in case of steels with higher yield strengths, e.g., above 700 MPa, locally undermatched regions can occur. Such an overmatched weld joint is quite sensitive to planar cracks developing from defects. Thus, a higher stress concentration around the planar defects in a weld metal in locally undermatched regions can cause unstable fracture behaviour[2]. In this case a significant range of experimentally fracture-toughness values is obtained. It is possible, however, to overcome this problem by determining the lower bound fracture toughness, which can ensure the structural integrity and a safe service life. The lower-bound fracture-toughness value represents the value where the crack propagation occurred. If the stress intensity factor (caused by applied load) is lower than the lower-bound fracture toughness, than crack propagation does not appear. This paper presents a procedure for determining the lower-bound fracture toughness of laboratory specimens cut from a critically overmatched weld joint. The influence of the weld-metal microstructure on the fracture behaviour is estimated, enabling an evaluation of the resistance to stable crack growth through different microstructures, as well as an evaluation of the relevant value of the lower bound of the fracture toughness. Reasons for the range of experimentally measured fracture-toughness values are also presented.

2 MATERIALS AND WELDING

The base metal is a high-strength low-alloy steel, corresponding to grade HT80. The steel, with a thickness of 40 mm, was delivered in quenched-and-tempered (Q + T) condition. Different mechanical properties can be obtained for such a steel by using different tempering temperatures (600–700 °C). The microstructure of the steel of tempered martensite and lower bainite provides a high strength and a high impact toughness. The welding was done on plate samples (500 × 250 × 40) mm and (1000 × 250 × 40) mm using the flux-cored arc-welding (FCAW) process. The edge preparation was X-shaped, **Figure 1**, as is usual for the welding of steel plates with a thickness of 40 mm. The consumables were filled wires (ϕ 1.2 mm), suitable for welding with mixed-gas shielding (82 % Ar and 18 % CO_2). The cooling times from 800 °C to 500 °C ($\Delta t_{8/5}$) were approximately of 9 s, with heat inputs of 1.8–2.0 MJ m^{-1}, while the preheating/inter-pass temperature was of 100 °C. The cooling time was chosen because faster cooling rates ($\Delta t_{8/5}$ = 6 s) reduce the toughness in the intercritical region, and the slower cooling rates ($\Delta t_{8/5}$ > 12 s) reduce the toughness due to the formation of a martensite-austenite constituent[3]. The welding parameters are given in **Table 1**. The first passes of the welded joint were made using preheating at 120 °C [4].
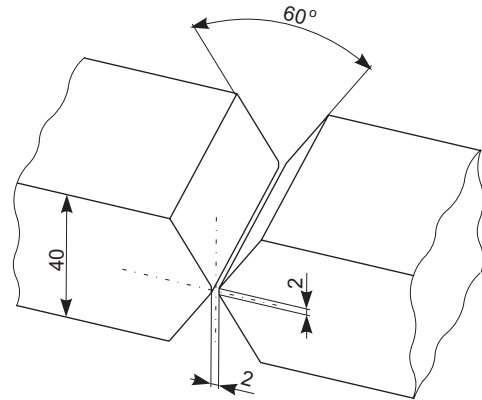
Figure 1: The "X" shaped groove used in this investigation
Slika 1: Žleb z X-obliko, uporabljen pri tej raziskavi

The chemical compositions of the base metal (BM) and the different weld regions are listed in **Table 2**. These compositions indicate a more pronounced alloying effect from the BM in the root region than in the filler regions. Local tempering or quenching caused by reheating and cooling during the deposition of subsequent passes is also present in the root and filler weld regions. This is the main reason why the local mis-matching through the weld thickness varied, even in the case of a homogeneous weld.

Table 1: Welding parameters for each weld pass
Tabela 1: Varilni parametri za vsak varek

Welding pass	Current A	Voltage V	Speed of welding cm/min	Interpass temperature °C	Heat input kJ/cm	$\Delta t_{8/5}$ s	Weld joint region
1	155	24.5	11.5	120	19.813	10.61	
2	185	23.5	13.7	135	19.040	10.82	root
3	250	24	16.0	30	22.500	8.78	
4	250	24	15.0	65	24.000	10.47	
5	240	23	10.5	105	31.543	15.65	
6	240	23	11.1	120	29.784	15.66	
7	220	23	15.9	65	19.130	8.43	
8	220	23.5	14.6	85	21.203	9.96	filler
9	210	23	14.2	120	20.481	10.95	part
10	220	23	13.9	125	21.763	11.83	
11	210	24	15.4	80	19.662	9.11	
12	250	24	14.8	110	24.342	12.43	
13	220	25	15.8	95	20.899	10.18	
14	230	25	19.5	125	17.692	9.70	
average	210	24	14.0	88	21.338	10.17	root
average	226	24	15.0	103	22.648	11.39	filler

Table 2: Chemical composition of the base metal, the pure weld metal and the actual weld metal of the filler and the root regions
Tabela 2: Kemična sestava osnovnega materiala, čistega vara, realnega vara v območju polnitve in korena v masnih deležih w/%

Material	C w/%	Si w/%	Mn w/%	P w/%	S w/%	Cr w/%	Ni w/%	Mo w/%	CE/%
Base metal	0.09	0.27	0.25	0.015	0.004	1.12	2.63	0.25	0.366
Weld metal (pure)	0.06	0.35	1.43	0.011	0.008	0.86	3.01	0.56	0.448
WM$_{fill}$ (filler part)	0.07	0.33	1.27	0.008	0.006	0.86	2.21	0.47	0.404
WM$_{root}$	0.08	0.32	0.78	0.012	0.007	0.99	2.50	0.35	0.388

The content of carbon is very low in the base metal and the weld metals and the temperature of martensite transformation is higher. Thus, the time interval for self-tempering from the temperature of martensite transformation up to room temperature is larger. In this case a brittle hard microstructure does not appear. This is the reason for the high toughness of the microstructure. **Table 2** presents the change of the carbon equivalent (CE) during the welding process. The low CE and the low strength hinder the hydrogen-assisted cold cracking. The mechanical properties of the welds were determined using round tensile specimens (ϕ 5 mm) extracted from the root and the cap region of the X-groove welds in longitudinal direction. The tensile tests were performed at room temperature and at the fracture-toughness testing temperature, i.e., –10 °C. The results are listed in **Table 3**, with the data in brackets representing the designed values (theoretical) of the mis-matching factor, which do not correspond to the real welds. The differences between the designed values and real mis-matching factors are a consequence of the weld-pool dilution/ alloying by molten BM (see chemical compositions in **Table 2**). It should also be pointed out that the cooling rate in these experiments ($\Delta t_{8/5} \approx 9$ s) was obviously different from that used during the all-weld metal sample preparation by the consumable producer.

Table 3: Average mechanical property values of the base metal and the weld metal
Tabela 3: Povprečne mehanske lastnosti osnovnega materiala in vara

Material	Temp. °C	E GPa	$R_{P0.2}$ MPa	R_m MPa	A_t %	Cv^+ J	M
Base	20°	201	711	838	19.6	54$_{-40 °C}$	–
metal	–10°	209	712	846	19	85$_{-10 °C}$	–
WM	20°	210*	770	845	16	56$_{-10 °C}$	(1.08)
WM$_{fill}$	20°	205	861	951	11.7	56$_{-10 °C}$	1.21
	–10°	211	873	1041	10.8	33$_{-40 °C}$	1.22
WM$_{root}$	20°	221	807	905	15.3	61$_{-10 °C}$	1.14
	–10°	212	824	902	16.5	50$_{-40 °C}$	1.16

+ mean value of three Charpy-V notched impact-toughness specimens
* value has been estimated because an accurate experimental value was not available

The impact-toughness V-notch specimens and the single-edge notch bend SE(B) specimens were also extracted from the welded joints. Different testing temperatures were used to evaluate the impact toughness. It can be concluded that the impact toughness corresponds to the brittle-to-ductile transition region of the weld joint, see **Table 3**. In spite of higher dilution/ alloying by the molten BM in the root region, a better impact toughness is achieved in that region than in the filler part of the WM.

The mis-match factor M is defined as:

$$M = \frac{\sigma_{y,\text{WM}}}{\sigma_{y,\text{BM}}} \qquad (1)$$

The mechanical properties listed in **Table 3** are the average values of the region from where the tensile specimens were taken. Hence, an empirical relationship was used to obtain the local mis-matching values of mechanical properties.

3 METALLOGRAPHIC INVESTIGATION

The cross-sections of the welded joints were polished and etched (3 % nital) to reveal the microstructure [5], shown in **Figure 2**. Previously performed fracture-toughness testing [6,7] showed that in the case of unstable crack propagation, the fracture-toughness value depended on the microstructure of the crack-tip region. Hence, a fracture-toughness analysis of unstable crack propagation requires the classification of the fracture toughness data connected to the microstructures at the crack tip.

Figure 3 shows a welded joint cross-section indicating two different regions inside a weld pass – one region, with a dendritic structure ('as-welded'), and the other one showing evidence of being re-heated at the subsequent welding pass. The darkened regions in the weld metal correspond to the partially transformed
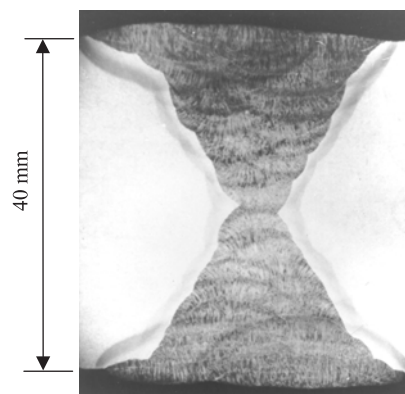
Figure 2: Macrograph of the cross-section of the welded joint, ×1.5
Slika 2: Makroposnetek prereza zvara, povečano 1,5-krat
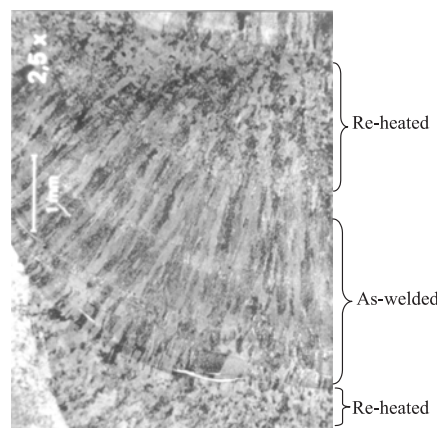
Figure 3: The re-heated and as-welded region within a welded pass, ×20
Slika 3: Pogreto in kot varjeno področje v varku, povečano 20-krat

regions, re-heated above Ac_1. The temperature of the subsequent weld pass was between Ac_1 and the self-tempering temperature.

4 FRACTURE-TOUGHNESS TESTING

Specimen and Location of Machined Notch

The critical crack-tip opening displacement (*CTOD*) value in the case of unstable crack propagation strongly depends on the microstructures at the crack tip. Different microstructures are formed in the weld metal, depending on the thermal cycles and the chemical composition. For this reason, the notch positioning in the welded joint is very important. The effect of different microstructure on the fracture behaviour was assessed by testing CTOD $B \times 2B$ specimens (thickness $B = 36$ mm) with a through-the-thickness notch tip in the weld metal. The CTOD $B \times B$ specimens, with the surface notch in the weld metal, were used to assess the effect of different microstructures on the fracture behaviour of the welded joint.

Crack-tip opening displacement testing

The fatigue pre-cracking of the specimens was performed according to the step-wise high-ratio R "SHR" technique [8]. The CTOD testing was performed on the fracture-toughness specimen in accordance with the BS 7448 standard [9]. The testing temperature was of –10 °C, according to the recommendations of the Offshore Mechanics and Arctic Engineering (OMAE) [10]. A single-specimen method was used with the DC potential-drop technique applied to monitor the stable crack growth [11]. The specimens were loaded using a constant cross-head velocity of 1 mm/min, i.e., in displacement control. Base-metal BxB specimens with a shallow crack ($a/W = 0.1$) and a deep crack ($a/W = 0.5$) were also tested. In both cases the maximum $CTOD_m$ values were observed: $CTOD_m = 1.08$ mm (for $a/W = 0.1$) and $CTOD_m = 0.604$ mm (for $a/W = 0.5$).

5 ANALYSIS OF THE FRACTURE-TOUGHNESS RESULTS

Figure 4 shows the resistance curves for almost the same crack lengths ($a/W = 0.27$), but with a different microstructure at the crack tip. The critical value of the CTOD during crack-growth initiation is lower for the 'as-welded' microstructure, denoted WM(B), than for the 're-heated' microstructure, denoted WM(A). The stable crack growth through WM(B) is characterised by a low slope of the resistance curve and thus by a low resistance to stable crack growth. The shallow-cracked specimen with a shorter crack ($a/W = 0.28$) exhibited a higher value of CTOD initiation than in the case of the longer crack ($a/W = 0.4$). In the latter case, local instability occurred ('pop-in') during crack-tip blunting, followed by crack arrest in the WM(A). The same slope
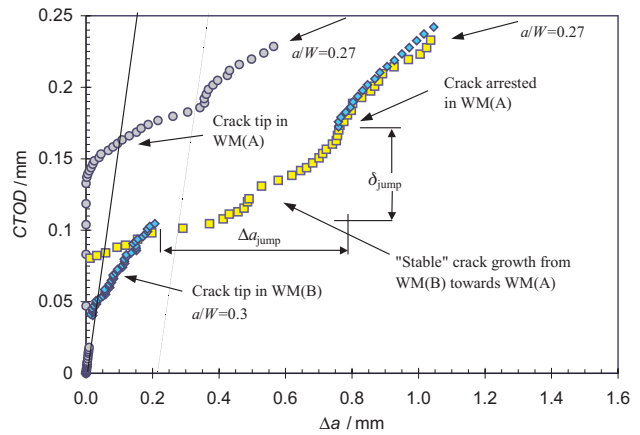

Figure 4: *CTOD* resistance curves of $B \times B$ specimens with the crack tip in different microstructure
Slika 4: *CTOD* odpornostne krivulje za $B \times B$ vzorce s konico razpoke v različni mikrostrukturi

for the resistance curves obtained from the two specimens with different crack lengths ($a/W = 0.27$ and $a/W = 0.4$) indicates to a stable crack growth through the same WM(A) microstructure.

Figure 5 shows the values of the CTOD as a fracture-toughness parameter for both series of specimens, $B \times 2B$ and $B \times B$, with the notch in the weld metal and the base metal. Significant differences between the fracture-toughness values of the base metal and weld metal were observed. Also, all critical values for the $B \times 2B$ specimens were within the same interval. This is a consequence from the incorporation of at least one local brittle zone (LBZ) or local soft region in the process zone in the vicinity of the crack tip.

The results for the critical CTOD, obtained using BxB specimens, are classified according to the microstructure, WM(A) and WM(B), depending on the position of the fatigue crack tip at the beginning of the CTOD testing. Since, the higher critical CTOD values were measured for the specimens with a crack tip in the WM(A), it is clear that the critical CTOD values for the specimens with a crack tip in the WM(B) can be divided
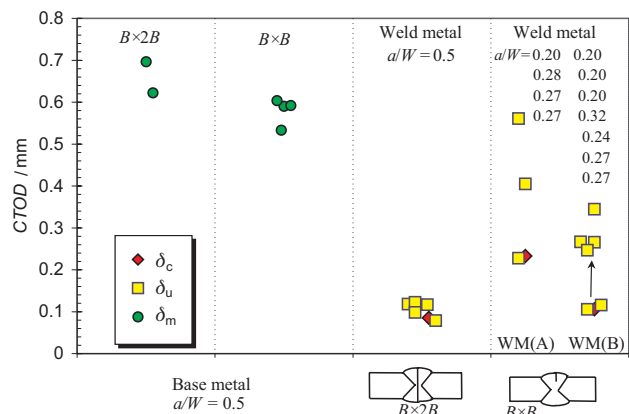

Figure 5: Compilation of the critical *CTOD* values
Slika 5: Pregled kritičnih vrednosti *CTOD*

into two groups, depending on the crack depth. Obviously, the scatter of the critical *CTOD* values and the relatively small amount of data prevented a more reliable estimation of the fracture-toughness lower-bound value for different microstructures.

A modified Weibull distribution was used for the statistical interpretation of the measured and corrected critical *CTOD* values. Zerbst et al. [12] proposed a modified Weibull distribution for estimating the lower-bound fracture toughness in terms of the J-integral [13]. The distribution function referring to this is given by:

$$P_f = \begin{cases} \dfrac{\sqrt{\ln 2}}{J_0}(J_C - J_{l.b.}), & P_f \leq 0.5 \\ 1 - \exp\left\{-\left[\dfrac{J_C}{J_0}\right]^2\right\}, & P_f \geq 0.5 \end{cases} \tag{2}$$

with the lower bound, $J_{l.b.}$, as the toughness for a failure probability of zero.

The term J can be replaced with $CTOD = \delta$ by using the relation between δ and J [14]:

$$d = \frac{J}{m \cdot \sigma_{ys}}$$

$$m = -0.111 + 0.817\frac{a}{W} + 1.36 \cdot R^*;$$

$$R^* = \left(\frac{500 \cdot n}{2.718}\right)^n \quad \text{or} \quad R^* = \frac{\sigma_m}{\sigma_y} \tag{3}$$

The terms **m** and **R*** were introduced by Kirk and co-workers [14] on the basis of finite-element analysis results. The lower bound fracture toughness can be derived by considering the condition of continuity for P_f. As a result, the lower bound is simply obtained from the mean value by the expression:

$$\delta_{l.b.} = 0.26 \cdot \beta \cdot \delta_{c,mean}$$

with

$$\beta = 1 + 2.737p - 2.327p^2 + 12580p^3 \tag{4}$$
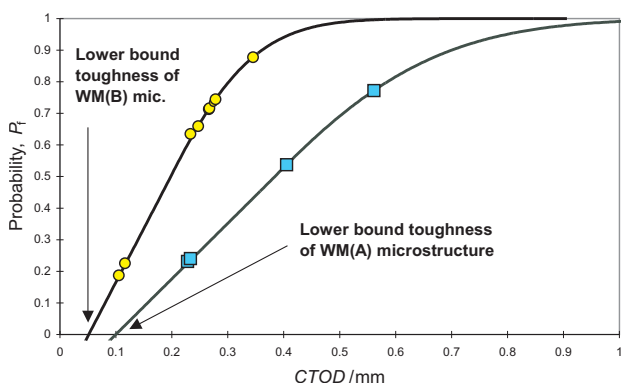
Figure 6: Failure probability with lower bound values classified by microstructures WM(A) and WM(B)
Slika 6: Verjetnost preloma pri spodnji vrednosti za mikrostrukturi WM(A) in WM(B)

where p is the fraction of data that is rejected by the size criterion.

The results of this analysis are two curves of Weibull distribution that are in good agreement with the experimental results for each individual microstructure, as shown in **Figure 6**. The lower-bound fracture-toughness value is represented by the CTOD value at the intersection point of the Weibull distribution curve with the *x*-axis. Although the Weibull distribution curves are for different microstructures, it is worth pointing out that the fracture-toughness lower-bound value is low for both of them [7].

6 CONCLUSION

In spite of the fact that the differences between the impact toughness of the weld metal and the base metal are insignificant, the fracture toughness of the weld metal can be significantly lower. The overmatched weld metal exhibited unstable crack propagation, while the base metal is ductile at the same test temperature. From the analysis performed on the B x B specimen it can be concluded that the critical value of the fracture toughness and the fracture behaviour of the weldment as a whole, depend on the crack depth and the microstructure at the crack tip, and also on the microstructure toward which the crack is growing. The influence of these parameters is reflected in pronounced differences in the experimentally obtained values. The higher reliability for estimating the fracture-toughness lower bound was achieved by using a modified Weibull distribution with the *CTOD* parameter. The B x 2B specimens also indicated low critical CTOD values, but with lower scatter. The reason for this is the increased constraint, since the ligament profile is of square shape, and also the fact that the stress state at the crack tip causes an interaction between strength-mis-matched microstructures, which are inevitably crossed by the crack front. In the case of through-the-thickness specimens at least one local brittle zone (LBZ) or a local soft region is incorporated in the process zone in the vicinity of the crack tip. Hence, the unstable fracture occurred with small stable crack propagation, or without. The statistically determined lower-bound fracture toughness takes account of this effect, which causes an increased scatter of experimental results. Therefore, for structural integrity procedures, it is possible to use the present approach to determine relevant fracture-toughness values.

7 REFERENCES

[1] Vojvodič Tuma J.: Low-temperature tensile properties, notch and fracture toughness of steels for use in nuclear power plants, Nuclear Engineering Design, (**2002**) 211, 105–119
[2] Gubeljak N.: The fracture behaviour of specimens with a notch tip partly in the base metal of strength mis-matched welded joints, Int. J. Fract., 100 (**1999**) 2, 169–181

[3] Matsuda, F., Fukada, Y., Okada, H., Shoga, C., Ikeuchi, K., Horii Y., Shiwaku, T., Suzuki, S.: Rewiew of mechanical and metallurgical investigations of martensite-austenite constituent in welded joints in Japan, Welding in the World, 37 (**1996**) 3, 134–154

[4] Duren C.: Evulation of large diametre pipe steel weldability by means of the carbon equivalent, Duisburg 1982

[5] Compendium of weld metal microstructures and properties (Submerged-arc welds in ferritic steel), Prepared for Commisssion IX of the International Institute of Welding by Sub-Commission IXJ, The Welding Institute Abington Hall, Cambridge UK 1985

[6] Machida, S., Miyata, T., Toyosada, M., Hagiwara, Y.: Study of methods for CTOD testing of weldments, fatigue and fracture testing of weldments, ASTM STP 1058, H. I. McHenry, J. M. Potter, Eds., American Society for Testing and Materials, Philadelphia, 1990, 142–156

[7] Fairchild, D. P.: Fracture toughness testing of weld heat-affected zones in structural steel, fatigue and fracture testing of weldments, ASTM STP 1058, H. I. McHenry, J. M. Potter, Eds., American Society for Testing and Materials, Philadelphia, 1990, 117–142

[8] Koçak M., Seifert, Yao S., Lampe H.: Comparison of fatigue precracking methods for fracture toughness testing of weldments: Local compression and step-wise high ratio, Conference Welding-90

[9] BS 7448 (1997): Fracture mechanics toughness tests, Part 2. Method for determination of KI, critical CTOD and critical J values of welds in metallic materials, British Standards Institution, London

[10] Fairchild, D. P., Theisen, J. D., Royer, C. P.: Philosophy and technique for assessing HAZ toughness of structural steels prior to steel production, Paper OMAE-88-910, Seventh International Conference on Offsore Mechanics and Artictic Engineering, Houston, TX, February 1988

[11] Johnson, H. H.: Calibrating the electric potential method for study slow crack growth, Materials Research and Standards, (**1965**) 5, 442–445

[12] Zerbst, U., Heerens, J., Puff, M., Wittkowsky, B. U., Schwalbe, K.-H.: Engineering estimation of the lower bound toughness in the transition regime of ferritic steels, Fatigue & Fracture of engineering materials & Structures, (**1998**) 21, 1273–1278

[13] Anderson, T. L.: Fracture mechanics fundamentals and applications, Second edition, 1994

[14] Kirk, M. T., Dodds, R. H.: J and CTOD estimation equations for shallow cracks in single edge notch bend specimens, J. of Testing and Evaluation, 21 (**1993**) 4